IET Control Theory & Applications

Research Article

Finite-time disturbance observer based integral sliding mode control for attitude stabilisation under actuator failure

ISSN 1751-8644
Received on 5th June 2018
Revised 25th August 2018
Accepted on 8th October 2018
E-First on 6th December 2018
doi: 10.1049/iet-cta.2018.5477
www.ietdl.org

Bo Li[1], *Qinglei Hu*[2] ✉, *Yongsheng Yang*[1], *Octavian Adrian Postolache*[1,3]

[1]*Institute of Logistics Science & Engineering, Shanghai Maritime University, Shanghai 201306, People's Republic of China*
[2]*School of Automation Science and Electrical Engineering, Beihang University, Beijing 100191, People's Republic of China*
[3]*Instituto de Telecomunicacoes, 1049-001 Lisbon, Portugal*
✉ *E-mail: huql_buaa@buaa.edu.cn*

Abstract: This work develops a novel disturbance observer and integral sliding mode technique based fault tolerant attitude control scheme for spacecraft, which is subject to external disturbance torques and actuator failures. More specifically, a simple and novel finite-time disturbance observer is first designed to reconstruct the synthetic uncertainty deriving from actuator failures and disturbances, by which the synthetic uncertainty is also compensated or restricted. Then, an integral sliding mode based finite-time fault tolerant attitude stabilisation controller incorporating with an adjusting law is investigated to ensure the closed-loop attitude control system converge to the stable region in finite time. And also the finite-time stability of the closed-loop attitude control system driven by the proposed attitude control scheme is analysed and proved utilising Lyapunov methodology. Finally, a simulation example for a rigid spacecraft model is carried out to verify the effectiveness and superiority of the proposed attitude control approach.

1 Introduction

Attitude control of spacecraft plays a very important role in many aerospace missions. And much attention has been paid by academic and industrial communities to their development, to ensure that the expected control system performance indices are achieved. Many control methods have been applied to achieve the attitude control missions, such as feedback control, non-linear control, optimal control, adaptive control, sliding mode control, robust control, and their integrations [1–7]. However, it may result in unsatisfactory performance even instability when unexpected malfunctions or catastrophic failures occur in actuating mechanisms. Therefore, fault tolerant control (FTC) and disturbance attenuation techniques must be taken into account for the construction of the spacecraft attitude control system.

In view of the existing researches, FTC methods can be classified into two main types, i.e. passive FTC (PFTC) and active FTC (AFTC). The PFTC aims at being robust against some known or expected types of failures by deteriorating the control system performances, such as the results in [8–10] and some correlative references therein. It is difficult for the above control law to react promptly, although it can finally counteract the faults or uncertainties through a passive feedback regulation in a relatively slow way. What is worse, it may lead to the control system instability in some abrupt or abominable situations. Thus, AFTC has attracted much attention in the past decades because of its feasibility and effectiveness to deal with the multiply or unknown failures. During the design of AFTC, fault detection and diagnosis (FDD) mechanism is a fundamental and essential part, which provides system failures or uncertainties information. FDD-based AFTC schemes have attracted considerable interests, especially for observer-based approaches, such as non-linear observer, robust observer, sliding mode observer, iterative learning observer, extended state observer (ESO) and so on [11–16]. Furthermore, in order to compensate for the lumped uncertainty/disturbance composed of external/internal disturbances and failures, disturbance observer (DO) has been considered as an effective way or an active approach to improve robustness, through estimating the lumped disturbance and designing DO-based controller [17–19]. In [19], a robust attitude tracking controller for quad-rotors based on the non-linear DO has been developed under parameter uncertainties and disturbance torques. In [20], the additive attitude measurement errors, external disturbances and system uncertainties are compensated by the non-linear DO during the design of backstepping based attitude stabilisation control approach. In order to offer superior convergence and better disturbance rejection capabilities, a hierarchical controller based on a new DO with finite-time convergence is proposed to solve the path tracking of a small coaxial-rotor-types unmanned aerial vehicles (UAVs) [21], and the unknown uncertainties and disturbances are reconstructed by the designed DO. However, the actuator failures are not taken into consideration during the design of the DO-based controllers.

Although the issue of spacecraft attitude control under actuator failures or system uncertainties has been researched and reported extensively, most works achieved asymptotic stability or bounded stability. As is known, finite-time control of dynamical system possesses the capacities of fast convergence, high-precise, and strong disturbance rejection and so on [22–25]. In [25], Du and Li investigates the finite-time attitude stabilisation problem for a rigid spacecraft with an unknown inertia matrix, and constructs a global finite-time stable control law. Gui *et al*. [26] designs several simple non-linear proportional-derivative type saturated finite-time controllers, but the disturbances and uncertainties cannot be taken into account.

To achieve the finite-time stability of the attitude control system under actuator failures or system uncertainties, sliding mode control (SMC) technique based FTC is recognised as an effective way. But, they have some disadvantages, for instance the system dynamics might be vulnerable to failures or uncertainties during the reaching phase in which the system states have not yet reached the sliding manifold [27]. To this end, integral type SMC (ISMC) has been developed such that the sliding mode starts from the initial time instant, which possesses the faster convergence speed and better robust performance due to the elimination of the reaching phase [27–29]. In [30], an ISMC-based fault tolerant controller is investigated to deal with the loss of failures of actuators. For the issue of attitude tracking control in the presence of inertia uncertainty, external disturbances and actuator failures, an ISMC-based adaptive fault tolerant attitude control approach is developed in [31]. However, they employ the passive/robust way to deal with the uncertainties and failures, and even the disturbance or chattering rejection problem is also not well addressed.

Motivated by addressing the above problems, this work investigates the finite-time DO (FTDO) and ISMC-based finite-time FTC of spacecraft attitude stabilisation. The control approach is developed in the framework of observer-based controller design, which achieves the following main contributions:

i. A simple novel FTDO is constructed to estimate and compensate for the synthetic uncertainty/disturbance deriving from actuator failures and disturbances. Although many other DOs have been presented for spacecraft, the proposed DO is simpler, which is just related to the observation error of the attitude angular velocity. On the other hand, the actuator failures are taken into consideration during the design of the DO-based control scheme in this work, which cannot be dealt with by the similar DO for the path tracking problem of a small coaxial-rotor-types UAVs in [21].
ii. An ISMC-based finite-time fault tolerant attitude controller incorporating with an adjusting law is investigated, to ensure the closed-loop attitude control system converge to the stable region in finite time. Although the utilised integral sliding mode surface in this work is inspired by [30], we have proposed the novel approaches including the design methods of finite-time observer and finite-time controller to handle the actuator failures and observation errors.

It should be highlighted that the whole spacecraft attitude control system including the DO and FTC mechanisms is verified to be finite-time stable. And also the system chattering problem has been well restrained such that the performances of strong robustness, high-reliability and high accuracy attitude stabilisation are achieved even in the presence of actuator failures and external disturbances simultaneously.

2 Spacecraft modelling and problem formulation

2.1 Spacecraft attitude kinematics

In this paper, the modified Rodrigues parameters (MRPs) based attitude representation method is utilised. Then, the spacecraft kinematics model is established as [32]

$$\dot{\boldsymbol{\rho}} = \boldsymbol{G}(\boldsymbol{\rho})\boldsymbol{\omega} \tag{1}$$

where the vector $\boldsymbol{\rho} \in \mathbf{R}^{3\times 1}$ is the attitude MRPs, and $\boldsymbol{G}(\boldsymbol{\rho}) = \left(\boldsymbol{I} - \boldsymbol{\rho}^{\times} + \boldsymbol{\rho}\boldsymbol{\rho}^{\mathrm{T}} - \left(\mathbf{1} + \boldsymbol{\rho}^{\mathrm{T}}\boldsymbol{\rho}\right)\boldsymbol{I}/\mathbf{2}\right)/2$. The vector $\boldsymbol{\omega} \in \mathbf{R}^{3\times 1}$ denotes the attitude angular velocity. Moreover, $\boldsymbol{I}$ is an identity unit matrix with the corresponding dimensions, and the symbol $(\cdot)^{\times}$ represents the operation to make a specified vector $(\cdot)$ to be a skew-symmetric matrix.

2.2 Spacecraft attitude dynamics

The dynamics of a rigid body are given by the following attitude rotational equation [32, 33]:

$$\boldsymbol{J}\dot{\boldsymbol{\omega}} = -\boldsymbol{\omega}^{\times}\boldsymbol{J}\boldsymbol{\omega} + \boldsymbol{u} + \boldsymbol{d} \tag{2}$$

where the matrix $\boldsymbol{J} \in \mathbf{R}^{3\times 3}$ denotes the positive-definite symmetric inertia matrix of the spacecraft, and $\boldsymbol{u} \in \mathbf{R}^{3\times 1}$ is the control torque. Whereas the vector $\boldsymbol{d} \in \mathbf{R}^{3\times 1}$ is the disturbance torque.

2.3 Actuator failure

Reaction wheel (RW) is the frequently-equipped actuator in aerospace engineering, which is also utilised to provide attitude stabilisation control torques in this work. As described in [16, 34], RWs are vulnerable to suffer the following four types of failures: F1, decreasing reaction torque; F2, continuous generation of reaction torque; F3, increasing bias torque; and F4, failure to react to the system control signals. Accordingly, the actual output torque can be modelled mathematically in the form of

$$\tau_i = e_{ii}v_i + \bar{v}_i \tag{3}$$

where $v_i (i = 1, 2, \ldots, m)$ is the desired control torque allocating to the individual actuator, $\bar{v}_i$ represents additive fault induced by F2 or F3, and $e_{ii} \in [0, 1]$ characterises the actuator control effectiveness. Then, the cases of failures can be categorised as (1) $e_{ii} = 1, \bar{v}_i = 0$ implies that the ith RW is working perfectly without any failure; (2) $0 < e_{ii} < 1, \bar{v}_i = 0$ indicates the ith RW undergoes F1; (3) $e_{ii} = 0, \bar{v}_i \neq 0$ indicates the ith RW undergoes F2; (4) $e_{ii} = 1, \bar{v}_i \neq 0$ shows the occurrence of F3; (5) $e_{ii} = 0, \bar{v}_i = 0$ implies completely failure of actuator.

Accordingly, the spacecraft dynamics with m actuators/RWs with failures are represented by

$$\boldsymbol{J}\dot{\boldsymbol{\omega}} = -\boldsymbol{\omega}^{\times}\boldsymbol{J}\boldsymbol{\omega} + \boldsymbol{D}\boldsymbol{v} + \bar{\boldsymbol{d}} \tag{4}$$

with $\bar{\boldsymbol{d}} = \boldsymbol{D}(\boldsymbol{E} - \boldsymbol{I})\boldsymbol{v} + \bar{\boldsymbol{v}} + \boldsymbol{d}$, which is the lumped/synthetic uncertainty or disturbance of the spacecraft attitude stabilisation system. Given spacecraft attitude stabilisation system is a typical over-actuated control system, the control allocation (CA) technique is one natural and necessary solution for achieving a desired control objective by distributing appropriately control signals synthesised to each individual actuator. $\boldsymbol{D} \in \mathbf{R}^{3\times m}$ is the configuration matrix or control allocation matrix, which should be full rank matrix for the requirements of the controllability of the over-actuated attitude control system in fault-free case. $\boldsymbol{E} = \mathrm{diag}(e_{11}, e_{22}, \ldots, e_{mm}) \in \mathbf{R}^{m\times m}$ denotes the actuator effectiveness matrix. It is noted that the number of actuators satisfying $e_{ii} \neq 0$ must be greater than three for the requirements of the controllability of the attitude control system as well. In addition, $\boldsymbol{v} = [v_1, v_2, \ldots, v_m]^{\mathrm{T}}$ and $\bar{\boldsymbol{v}} = [v_1, v_2, \ldots, v_m]^{\mathrm{T}}$ are the commanded/desired torque and additive output vectors, respectively.

Assumption 1: The output torque magnitudes of the actuators installed in spacecraft are assumed to subject to the same constraint value, which is noted as $\tau_{\max}$ for simplicity.

Assumption 2: The lumped disturbance torque term $\bar{\boldsymbol{d}}$ in (4) is supposed to be bounded and differentiable. In addition, with respect to Assumption 1 and the actuators' failures referred above, the additive torque of the individual actuator $\bar{v}_i$ is also bounded. Therefore, it is reasonable to suppose that there always exists a constant $\bar{d}_1$ such that $\|\bar{\boldsymbol{d}}\| \leq \bar{d}_1$.

3 FTDO based attitude stabilisation control

3.1 Preliminaries

For the convenience and simplicity of the mathematical descriptions, some notations are defined as follows:

$$\begin{aligned}\mathrm{sig}^{\alpha}(\boldsymbol{x}) &= \mathrm{sign}(\boldsymbol{x})|\boldsymbol{x}|^{\alpha}\\ &= \left[\mathrm{sign}(x_1)|x_1|^{\alpha}, \mathrm{sign}(x_2)|x_2|^{\alpha}, \ldots, \mathrm{sign}(x_n)|x_n|^{\alpha}\right]^{\mathrm{T}},\end{aligned}$$

$$|\boldsymbol{x}|^{\alpha} = \left[|x_1|^{\alpha}, |x_2|^{\alpha}, \ldots, |x_n|^{\alpha}\right]^{\mathrm{T}},$$

where $\boldsymbol{x} = [x_1, x_2, \ldots, x_n]^{\mathrm{T}}$, $0 < \alpha < 1$. $\mathrm{sign}(x)$ denotes a sign function for the variable x, which is defined as

$$\mathrm{sign}(x) = \begin{cases} 1, & x > 0; \\ 0, & x = 0; \\ -1, & x < 0. \end{cases}$$

Then, consider the following non-linear system:

$$\dot{\boldsymbol{x}}(t) = f(\boldsymbol{x}(t)), \quad \boldsymbol{x}(0) = \boldsymbol{x}_0, \quad f(0) = 0, \quad \boldsymbol{x} \in \mathbf{R}^n \tag{5}$$

where $f: \boldsymbol{U} \to \mathbf{R}^n$ is continuous in an open neighbourhood $\boldsymbol{U}$ of the origin. Suppose that the system in (5) possesses a unique solution in forward time for all initial conditions.

Definition 1 (Finite-time stability [22]): If the non-linear system (5) is Lyapunov stable, the equilibrium $\boldsymbol{x} = 0$ is constantly established in finite time, then (5) is finite-time stable in an open neighbourhood $\boldsymbol{U}_0 \subset \boldsymbol{U}$. The finite-time convergence means the existence of a function $T: \boldsymbol{U}_0 \setminus \{0\} \to (0, \infty)$, such that $\forall \boldsymbol{x}_0 \in \boldsymbol{U}_0 \setminus \{0\}$, the solution of the above system $\boldsymbol{s}_f(t, \boldsymbol{x}_0) \in \boldsymbol{U}_0 \setminus \{0\}$ for $t \in [0, T(\boldsymbol{x}_0)]$, and $\lim_{t \to T(\boldsymbol{x}_0)} \boldsymbol{s}_f(t, \boldsymbol{x}_0) = 0$. If the zero solution is finite-time convergent, the set of point $\boldsymbol{x}_0$ such that $\boldsymbol{s}_f(t, \boldsymbol{x}_0) \to 0$ is called the domain of attraction of the solution. When $\boldsymbol{U} = \mathbf{R}^n$, one can achieve that the equilibrium is globally stable in finite time.

Definition 2 (Practically finite-time stability [35]): For all the initial value $\boldsymbol{x}_0$, if there exists $\epsilon > 0$ and $T(\epsilon, \boldsymbol{x}_0) < \infty$ such that the system states meet $\| \boldsymbol{x} \| < \epsilon$ for all the time $t \leq t_0 + T$, the non-linear system (5) is practically finite-time stable, or finite-time uniformly ultimately bounded stable.

Lemma 1 (Locally finite-time stability [21, 22, 36]): Consider the non-linear system (5), and suppose there exists a Lyapunov function $V(\boldsymbol{x})$ defined on a neighbourhood $\boldsymbol{U} \subset \mathbf{R}^n$ of the origin, and $\dot{V}(\boldsymbol{x}) + \beta_1 V(\boldsymbol{x})^{\alpha_1} < 0$ with $\boldsymbol{x} \in \boldsymbol{U} \setminus \{\boldsymbol{0}\}$, $0 < \alpha_1 < 1$, $\beta_1 > 0$. Then, (5) is locally finite-time stable (LFTS), and the needed time to reach the target $V(\boldsymbol{x}) = 0$ is $T \leq (1/(\beta_1(1 - \alpha_1))|V(\boldsymbol{x}_0)|^{1-\alpha_1}$, in which $V(\boldsymbol{x}_0)$ denotes the initial value of $V(\boldsymbol{x})$.

Lemma 2 (Practically finite-time stability or finite-time uniformly ultimately bounded stability [35, 37]): Consider the non-linear system (5), and suppose there exists a Lyapunov function $V(\boldsymbol{x})$ such that $\dot{V}(\boldsymbol{x}) \leq -\beta_1 V(\boldsymbol{x})^{\alpha_1} + \eta$ with $0 < \alpha_1 < 1$, $\beta_1 > 0$, and $0 < \eta < \infty$. Then the trajectory of system is practically finite-time stable or finite-time uniformly ultimately bounded stable. It means that the system states $\boldsymbol{x}$ could converge to a small set around the equilibrium in the finite time T. The settling time is subject to $T \leq (1/((\beta_1 - \theta))(1 - \alpha_1)|V(\boldsymbol{x}_0)|^{1-\alpha_1}$ with $\theta \in (0, \beta_1)$. And the residual set of the solution of the system (5) is bounded as $\lim_{t \to T} \boldsymbol{x} \in \left(V(\boldsymbol{x})^{\alpha_1} \leq \eta/\theta\right)$.

Proposition 1 (Proposition of the finite-time uniformly ultimately bounded stability given in Lemma 2 [36, 37]): Consider the same system in (5) and an existing Lyapunov function $V(\boldsymbol{x})$. The trajectory of the system is finite-time uniformly ultimately bounded stable in the region of $Q = \{\boldsymbol{x} \,|\, V(\boldsymbol{x})^{\alpha_1 - \alpha_2} < (\beta_2/\theta_1)\}$, if $\dot{V}(\boldsymbol{x}) \leq -\beta_1 V(\boldsymbol{x})^{\alpha_1} + \beta_2 V(\boldsymbol{x})^{\alpha_2}$ for $\alpha_1 > \alpha_2$, $\beta_1 > 0$, $\beta_2 > 0$, $\theta_1 \in (0, \beta_1)$. The settling time for the states reaching the stable residual set is bounded as $T \leq [(V(\boldsymbol{x}_0)^{1-\alpha_1})/((\beta_1 - \theta_1)(1 - \alpha_1))]$.

Lemma 3 (Globally finite-time stability [24, 26]): Consider the following system:

$$\dot{\boldsymbol{x}} = \boldsymbol{f}(\boldsymbol{x}) + \hat{\boldsymbol{f}}(\boldsymbol{x}), \quad \boldsymbol{f}(0) = 0, \quad \boldsymbol{x} \in \mathbf{R}^n \tag{6}$$

where $\boldsymbol{f}(\boldsymbol{x})$ is a continuous homogeneous vector field of degree $k < 0$ with respect to a dilation $\Delta_\epsilon^{\boldsymbol{r}}$ defined by $\Delta_\epsilon^{\boldsymbol{r}} \boldsymbol{x} = \left[\epsilon^{r_1} x_1, \epsilon^{r_2} x_2, \ldots, \epsilon^{r_n} x_n\right]$, $\boldsymbol{r} = (r_1, r_2, \ldots, r_n)$, and the perturbation vector field $\hat{\boldsymbol{f}}(\boldsymbol{x})$ satisfies $\hat{\boldsymbol{f}}(0) = 0$. If the system (6) is both globally asymptotic stable (GAS) and LFTS, then it is globally finite-time stable (GFTS).

3.2 FTDO design

The FTDO dynamics for the attitude stabilisation control system in (4) is established as

$$\boldsymbol{J}\dot{\hat{\boldsymbol{\omega}}} = -\boldsymbol{\omega}^{\times}\boldsymbol{J}\boldsymbol{\omega} + \boldsymbol{D}\boldsymbol{v} + \boldsymbol{\vartheta} \tag{7}$$

where $\boldsymbol{\vartheta}$ is an auxiliary variable which will be designed thereinafter. Let $\hat{\boldsymbol{\omega}}$ be the observed value of the attitude angular velocity $\boldsymbol{\omega}$, and denote $\tilde{\boldsymbol{\omega}} = \boldsymbol{\omega} - \hat{\boldsymbol{\omega}}$ as the observation error. In view of (4) and (7), the observation error dynamics could be written as

$$\dot{\tilde{\boldsymbol{\omega}}} = \boldsymbol{J}^{-1}\bar{\boldsymbol{d}} - \boldsymbol{J}^{-1}\boldsymbol{\vartheta} \tag{8}$$

$$\boldsymbol{\vartheta} = \lambda_1 \boldsymbol{J} \,\mathrm{sig}^{\alpha_1}(\tilde{\boldsymbol{\omega}}) + \lambda_2 \boldsymbol{J} \int \mathrm{sig}^{\alpha_2}(\tilde{\boldsymbol{\omega}}(\ell))\mathrm{d}\ell \tag{9}$$

with $\alpha_1 \in (1/2, 1)$, $\alpha_2 = 2\alpha_1 - 1$, $\lambda_1 > 0$ and $\lambda_2 > 0$.

Consider the following transformation of coordinates:

$$\boldsymbol{z} = [\boldsymbol{z}_1, \boldsymbol{z}_2]^{\mathrm{T}} = [\tilde{\boldsymbol{\omega}}, \boldsymbol{\xi}]^{\mathrm{T}} \tag{10}$$

with $\boldsymbol{\xi} = -\lambda_2 \int \mathrm{sig}^{\alpha_2}(\tilde{\boldsymbol{\omega}}(\ell))\mathrm{d}\ell + \boldsymbol{J}^{-1}\bar{\boldsymbol{d}}$. Then, one can obtain

$$\dot{\boldsymbol{z}}_1 = -\lambda_1 \,\mathrm{sig}^{\alpha_1}(\boldsymbol{z}_1) + \boldsymbol{z}_2 \tag{11a}$$

$$\dot{\boldsymbol{z}}_2 = -\lambda_2 \,\mathrm{sig}^{\alpha_2}(\boldsymbol{z}_1) + \boldsymbol{g}(t) \tag{11b}$$

where $\boldsymbol{g}(t)$ is the differential of the first term in (8) with respect to time. It is assumed to be bounded by $\| \boldsymbol{g}(t) \| \leq g_1$, in which g_1 is an existing and known constant. In view of this, the following statement can be obtained as the first achievement of this work.

Theorem 1: Consider the spacecraft system in (1) and (4) under Assumptions 1 and 2, applying the proposed FTDO mechanism in (7)–(9) with appropriate gains, the states $\boldsymbol{z}_1$ and $\boldsymbol{z}_2$ in the auxiliary system in (11) are finite-time uniformly ultimately bounded stable. Then $\dot{\boldsymbol{z}}_1$ converges to a small region of the origin in finite time, which also implies that the auxiliary variable $\boldsymbol{\vartheta}$ will converge to the synthetic uncertainty $\bar{\boldsymbol{d}}$ in finite time.

Proof of Theorem 1: Define the following positive-definite Lyapunov function as:

$$V_1 = \boldsymbol{\varepsilon}^{\mathrm{T}} \boldsymbol{P} \boldsymbol{\varepsilon} \tag{12}$$

where the vector $\boldsymbol{\varepsilon}$ and the symmetric positive definite matrix $\boldsymbol{P}$ are defined, respectively, as

$$\boldsymbol{\varepsilon} = \left[\mathrm{sig}^{\alpha_1}(\boldsymbol{z}_1), \boldsymbol{z}_2\right]^{\mathrm{T}}, \quad \boldsymbol{P} = \frac{1}{2\alpha_1}\begin{bmatrix} 2\lambda_2 + \alpha_1\lambda_1^2 & -\alpha_1\lambda_1 \\ -\alpha_1\lambda_1 & 2\alpha_1 \end{bmatrix}.$$

Note that the designed Lyapunov candidate function in (12) is continuous and differentiable except on the set $\mathscr{Z}_1 = \{(\boldsymbol{z}_1, \boldsymbol{z}_2) \,|\, \boldsymbol{z}_1 = 0\}$, it yields to

$$\lambda_{\min}(\boldsymbol{P}) \| \boldsymbol{\varepsilon} \|^2 \leq V_1 \leq \lambda_{\max}(\boldsymbol{P}) \| \boldsymbol{\varepsilon} \|^2 \tag{13}$$

in which $\lambda_{\max}(\cdot)$ and $\lambda_{\min}(\cdot)$ represent the maximum and minimum eigenvalues of the specified matrix, respectively.

By proceeding with differentiation of the Lyapunov function V_1 with respect to time, one can obtain that

$$
\begin{aligned}
\dot{V}_1 &= \frac{1}{\alpha_1}[\mathrm{sig}^{\alpha_1}(z_1), z_2]\begin{bmatrix} 2\lambda_2+\alpha_1\lambda_1^2 & -\alpha_1\lambda_1 \\ -\alpha_1\lambda_1 & 2\alpha_1 \end{bmatrix} \\
&\cdot \begin{bmatrix} \alpha_1|z_1|^{\alpha_1-1}\left(-\lambda_1\mathrm{sig}^{\alpha_1}(z_1)+z_2\right) \\ -\lambda_2\mathrm{sig}^{\alpha_2}(z_1)+\boldsymbol{g} \end{bmatrix} \\
&\le -\|z_1\|^{\alpha_1-1}\left[\left(\lambda_2+\alpha_1\lambda_1^2\right)\lambda_1\mathrm{sig}^{2\alpha_1}(z_1)\right. \\
&\quad \left. +\alpha_1\alpha_2 z_2^2 - 2\lambda_1^2\alpha_1\mathrm{sig}^{\alpha_1}(z_1)z_2\right] \\
&\quad +\boldsymbol{\varepsilon}^{\mathrm{T}}\begin{bmatrix} -\lambda_1 \\ 2 \end{bmatrix}\boldsymbol{g} \\
&\le -\|z_1\|^{\alpha_1-1}\boldsymbol{\varepsilon}^{\mathrm{T}}\boldsymbol{Q}\boldsymbol{\varepsilon}+\boldsymbol{\varepsilon}^{\mathrm{T}}\boldsymbol{r}\boldsymbol{g}
\end{aligned}
\tag{14}
$$

with

$$
\boldsymbol{Q} = \lambda_1\begin{bmatrix} \lambda_2+\alpha_1\lambda_1^2 & -\alpha_1\lambda_1 \\ -\alpha_1\lambda_1 & \alpha_1 \end{bmatrix}, \quad \boldsymbol{r} = \begin{bmatrix} -\lambda_1 \\ 2 \end{bmatrix}.
$$

According to the definition of $\boldsymbol{\varepsilon}$ in (12), one can obtain that

$$
\|z_1\|^{\alpha_1-1} \ge \|\boldsymbol{\varepsilon}\|^{((\alpha_1-1)/\alpha_1)}. \tag{15}
$$

Further, the differential of V_1 in (14) follows that

$$
\begin{aligned}
\dot{V}_1 &\le -\|z_1\|^{\alpha_1-1}\lambda_{\min}(\boldsymbol{Q})\|\boldsymbol{\varepsilon}\|^2+g_1\|\boldsymbol{\varepsilon}\|\|\boldsymbol{r}\| \\
&\le -\lambda_{\min}(\boldsymbol{Q})\|\boldsymbol{\varepsilon}\|^{((\alpha_1+\alpha_2)/\alpha_1)}+g_1\|\boldsymbol{r}\|\|\boldsymbol{\varepsilon}\| \\
&\le -\lambda_{\min}(\boldsymbol{Q})\lambda_{\max}(\boldsymbol{P})^{-((\alpha_1+\alpha_2)/2\alpha_1)}V_1^{((\alpha_1+\alpha_2)/(2\alpha_1))} \\
&\quad +g_1\|\boldsymbol{r}\|\lambda_{\min}(\boldsymbol{P})^{-(1/2)}V_1^{1/2} \\
&\le -M_1V_1^{((\alpha_1+\alpha_2)/2\alpha_1)}+M_2V_1^{1/2}
\end{aligned}
\tag{16}
$$

where $\bar{\alpha} = (\alpha_1+\alpha_2)/2\alpha_1$, $M_1 = \lambda_{\min}(\boldsymbol{Q})\lambda_{\max}(\boldsymbol{P})^{-((\alpha_1+\alpha_2)/2\alpha_1)}$, and $M_2 = g_1\|\boldsymbol{r}\|\lambda_{\min}(\boldsymbol{P})^{-(1/2)}$. Given the variables $\alpha_1 \in (1/2, 1)$ and $\alpha_2 = 2\alpha_1 - 1$, one can obtain easily that $\bar{\alpha} \in (1/2, 1)$. That is to say, the fractional powers in the inequality (16) meet the following relationship $\bar{\alpha} > 1/2$. According to Proposition 1, the finite-time uniformly ultimately bounded stability of the auxiliary system in (11) can be established, which indicates that the states z_1 and z_2 in (11) will converge to the small region as

$$
D_0 = \left\{\boldsymbol{\varepsilon} \,|\, V(\boldsymbol{\varepsilon}) < \left(\frac{M_2}{\theta_1}\right)^{2\alpha_1/\alpha_2}\right\} \tag{17}
$$

with $\theta_1 \in (0, M_1)$. And the settling time for the states reaching the stable residual set is bounded as $T_0 \le [(V(\boldsymbol{\varepsilon}_0))^{1-\bar{\alpha}})/((M_1-\theta_1)(1-\bar{\alpha}))]$. It also implies that the auxiliary variable $\boldsymbol{\vartheta}$ is bounded, and it will converge to the synthetic uncertainty $\bar{\boldsymbol{d}}$ in finite time. Then, the reconstruction error of the synthetic failure/uncertainty $\boldsymbol{\vartheta}$ deriving from FTDO is bounded theoretically in finite time, and the upper bound is assumed to be $\boldsymbol{\varrho} = [\varrho_1, \varrho_2, \varrho_3]$. This completes the proof. □

3.3 Finite-time attitude stabilisation controller design

In this subsection, a simple finite time control law is first developed for the zero-disturbance and fault-free attitude stabilisation control system, which also will be used as a baseline controller in the next subsection for the FTC design.

Theorem 2: Consider the spacecraft system in (1) and (4) under Assumptions 1 and 2 without any actuator faults and external disturbances

$$
\boldsymbol{J}\dot{\boldsymbol{\omega}} = -\boldsymbol{\omega}^{\times}\boldsymbol{J}\boldsymbol{\omega}+\boldsymbol{D}\boldsymbol{v}, \tag{18}
$$

the finite time stable of the spacecraft attitude can be established if the control law is designed as

$$
\boldsymbol{v}_{nm} = \boldsymbol{D}^{\dagger}\left(-k_1\boldsymbol{G}^{\mathrm{T}}(\boldsymbol{\rho})\,\mathrm{sig}^{\beta_1}(\boldsymbol{\rho}) - k_2\,\mathrm{sat}_{\beta_2}(\boldsymbol{\omega})\right), \tag{19}
$$

where the control gains are subject to the constraints $k_1 > 0$, $k_2 > 0$, $0 < \beta_1 < 1$, $\beta_2 = 2\beta_1/(1+\beta_1)$; $\boldsymbol{D}^{\dagger} = \boldsymbol{D}^{\mathrm{T}}(\boldsymbol{D}\boldsymbol{D}^{\mathrm{T}})^{-1}$ is the pseudo-inverse of the control allocation matrix $\boldsymbol{D}$; $\mathrm{sat}_{\beta_2}(\cdot)$ is a new type of saturation function, which is defined as

$$
\mathrm{sat}_{\beta_2}(x) = \begin{cases} \mathrm{sig}^{\beta_2}(x), & \text{if } |x| \le 1; \\ \mathrm{sign}(x), & \text{otherwise.} \end{cases} \tag{20}
$$

Proof of Theorem 2: According to Lemma 3, the proof of Theorem 2 proceeds in two steps: (1) the GAS of the spacecraft attitude control system is firstly proven by the following Lyapunov method and involking LaSalle invariance principle, (2) then the LFTS is shown using homogeneity system theory.

Step 1. GAS analysis: We consider the Lyapunov candidate function as follows:

$$
V_2 = \frac{1}{2}\boldsymbol{\omega}^{\mathrm{T}}\boldsymbol{J}\boldsymbol{\omega} + \frac{k_1}{1+\beta_1}\sum_{i=1}^{3}\left|\rho_i\right|^{1+\beta_1}. \tag{21}
$$

By proceeding with differentiation of V_2 in (21), one can achieve

$$
\begin{aligned}
\dot{V}_2 &= \boldsymbol{\omega}^{\mathrm{T}}\left(-\boldsymbol{\omega}^{\times}\boldsymbol{J}\boldsymbol{\omega}+\boldsymbol{D}\boldsymbol{v}+\bar{\boldsymbol{d}}\right)+k_1\dot{\boldsymbol{\rho}}\,\mathrm{sig}^{\beta_1}(\boldsymbol{\rho}) \\
&= -\boldsymbol{\omega}^{\mathrm{T}}k_2\,\mathrm{sat}_{\beta_2}(\boldsymbol{\omega}) \le 0.
\end{aligned}
\tag{22}
$$

Then, one can obtain a conclusion that V_2 is positive-definite and its differentiation $\dot{V}_2$ is a negative semi-definite function. Since $\dot{V}_2 \equiv 0$ implies $\boldsymbol{\omega} \equiv \boldsymbol{0}$, one has $\boldsymbol{\rho} \equiv \boldsymbol{0}$ from the kinematics and dynamics of the spacecraft attitude control system. By LaSalle invariance principle, the GAS of the attitude control system is established.

Step 2. GFTS analysis: The LFTS of the attitude control system can be proven using finite-time stable lemmas associated with homogeneity theory. The proof process can be achieved by the similar method in [25, 26], which is omitted here for space limitation. □

3.4 Integral-type sliding mode based finite-time fault tolerant attitude stabilisation controller design

For the fine control performance, a novel ISMC-based fault tolerant controller incorporating with a dynamical adjusting law (noted as ISMFTC) is investigated for the spacecraft attitude control system with actuator failures and external disturbances in this subsection, with the help of the developed FTDO mechanism in (7)–(9).

Utilising the ISMC approach [30], the sliding manifold is first introduced in the form of

$$
\begin{aligned}
\boldsymbol{s} = \boldsymbol{P}\Big\{&\boldsymbol{\omega}(t)-\boldsymbol{\omega}(t_0) \\
&-\int_{t_0}^{t}\boldsymbol{J}^{-1}\left(-\boldsymbol{\omega}(\ell)^{\times}\boldsymbol{J}\boldsymbol{\omega}(\ell)+\boldsymbol{D}\boldsymbol{v}_{nm}(\boldsymbol{\rho},\boldsymbol{\omega})\right)\mathrm{d}\ell\Big\},
\end{aligned}
\tag{23}
$$

where $\boldsymbol{P} \in \mathbf{R}^{3\times 3}$ is a positive definite constant matrix, which should be designed such that $\boldsymbol{P}\boldsymbol{J}^{-1}$ is invertible. In view of (23), $\boldsymbol{s}(\boldsymbol{\omega}(t_0), t_0) = 0$ can be guaranteed at the time $t = t_0$. It implies that the reaching phase is eliminated due to the specific construction of the presented ISMC [30, 38].

Taking the differential of (23), it yields to

$$
\dot{\boldsymbol{s}} = \boldsymbol{P}\boldsymbol{J}^{-1}\left(\boldsymbol{D}\boldsymbol{v} - \boldsymbol{D}\boldsymbol{v}_{nm} + \bar{\boldsymbol{d}}\right), \tag{24}
$$

Then, one can obtain the equivalent control law by solving the equation $\dot{\boldsymbol{s}} = 0$, which is

$$
\boldsymbol{v}_{eq} = \boldsymbol{v}_{nm} - \boldsymbol{D}^{\dagger}\bar{\boldsymbol{d}}, \tag{25}
$$

Submitting the equivalent controller in (25) into the spacecraft dynamics in (4), one can achieve the sliding mode dynamics as

$$\boldsymbol{J}\dot{\boldsymbol{\omega}}_{eq} = -\boldsymbol{\omega}_{eq}^{\times}\boldsymbol{J}\boldsymbol{\omega}_{eq} + \boldsymbol{u}_{nm}\,. \tag{26}$$

where the subscript *eq* denotes the state vector on the sliding mode. Therefore, the finite-time stability of the sliding dynamics in (26) is can be established by using the equivalent control design approach according to Theorem 2.

For meeting the requirements of practical engineering, such as fast convergence, robustness, and high steady-state precision and so on, the construction of the FTC is developed as

$$\boldsymbol{v} = \boldsymbol{v}_{nm} + \boldsymbol{v}_{ns}, \tag{27}$$

where $\boldsymbol{v}_{nm}$ is the normal/baseline control signal designed in (20), which determines the behaviour of the nominal system restricted onto the sliding manifold. Whereas, the other control component $\boldsymbol{v}_{ns}$ consists of the robust control component compensating for the synthetic uncertainty and the finite-time control term forcing the attitude control system to converge to the origin in finite time. Based on the ISMC and adaptive techniques, another main contribution of this work states as follows.

Theorem 3: Consider the attitude control system in (1) and (4) under Assumptions 1 and 2 in the presence of actuator failures and disturbances. If the integral-type sliding manifold (23) based control law is developed as (27), i.e. $\boldsymbol{v} = \boldsymbol{v}_{nm} + \boldsymbol{v}_{ns}$, with

$$\boldsymbol{v}_{ns} = \boldsymbol{D}^{\dagger}\left(-\boldsymbol{\vartheta} - \hat{\boldsymbol{\varrho}}\,\mathrm{sign}(\boldsymbol{s}) - \boldsymbol{K}_3\boldsymbol{s} - \boldsymbol{K}_4\,\mathrm{sig}^{\gamma}(\boldsymbol{s})\right) \tag{28}$$

and the parameter adjusting laws are

$$\dot{\hat{\varrho}}_i = \begin{cases} \zeta_{1i}|s_i|^{\kappa_\epsilon(s_i)}\,\mathrm{sgn}(|s_i| - \epsilon_i), & \text{if } \hat{\varrho}_i > \mu; \\ \zeta_{2i}|s_i|, & \text{otherwise}, \end{cases} \tag{29}$$

the integral-type sliding manifold in (23) will reach the real sliding mode $|s_i| < \epsilon_i$ within finite time. Then the attitude control system is also practically finite-time stable or finite-time uniformly ultimately bounded stable. In (29), $\kappa_\epsilon(s_i) = 0.5 + 0.5\,\mathrm{sat}(4|s_i| - 3\epsilon_i/\epsilon_i)$, and $\mathrm{sat}(\cdot)$ is a widely-used saturation function, which is defined as

$$\mathrm{sat}(x) = \begin{cases} 1, & x > 1; \\ x, & -1 \le x \le 1; \\ -1, & x < -1\,. \end{cases}$$

The adaptive parameter $\hat{\boldsymbol{\varrho}} = \mathrm{diag}(\hat{\varrho}_i)$ is the estimation of the upper bound $\boldsymbol{\varrho}$, which is of the reconstruction error of the synthetic failure/uncertainty deriving from FTDO in Section 3.2. Whereas, $\boldsymbol{K}_3 = \mathrm{diag}(k_{3i})$ and $\boldsymbol{K}_4 = \mathrm{diag}(k_{4i})$ denote symmetric positive-definite control gain matrices. $\zeta_{1i} > 0$ and $\zeta_{2i} > 0$ $(i = 1, 2, 3)$ are dynamic gain parameters deciding the variation/developing of the adaptive parameter $\hat{\varrho}_i$, while $\mu > 0$ and $\epsilon_i > 0$ are small constants. Additionally, the initial value of the parameter adaptive law in (29) should be positive and greater than μ to achieve fine control performance.

To proof and analysis the above Theorem 3, the following lemma is firstly introduced [16, 39, 40].

Lemma 4: Consider the spacecraft attitude control system in (1) and (4), controlled by the proposed control schemes in (27)–(29) with the integral-type sliding mode manifold in (23) satisfying $|s_i| \neq 0$, the adjusting parameter $\hat{\varrho}_i$ has an upper-bound, i.e. there exists a positive constant ϱ_i^* such that $\hat{\varrho}_i \le \varrho_i^*$ and $\varrho_i \le \varrho_i^*$ are established all the time.

Proof of Lemma 4: Consider a Lyapunov candidate function as

$$V_3 = \frac{1}{2}\left(\boldsymbol{s}^{\mathrm{T}}\boldsymbol{J}\boldsymbol{P}^{-1}\boldsymbol{s} + \sum_{i=1}^{3}\frac{1}{\ell_i}\tilde{\varrho}_i^2\right) \tag{30}$$

where $\tilde{\varrho}_i = \varrho_i - \hat{\varrho}_i$ denotes the estimation error; and ℓ_i is a positive parameter, which has nothing to do with the control performance. By differentiating V_3 along with the control schemes (27)–(29), the proof process can be analysed in three cases. That is,

1. $\hat{\varrho}_i > \mu$ and $|s_i| \ge \epsilon_i$,
2. $\hat{\varrho}_i > \mu$ and $|s_i| < \epsilon_i$,
3. $\hat{\varrho}_i \le \mu$.

When $\hat{\varrho}_i > \mu$ (cases 1 and 2), $\hat{\varrho}_i$ is bounded and will be monotonically decreasing. Once $\hat{\varrho}_i$ goes into the region of $\hat{\varrho}_i \le \mu$, one also can obtain that $\dot{V}_3 \le 0$ by choosing appropriate parameter values to meet $\zeta_{2i} = \ell_i$. It should be noted that $\dot{V}_3$ may be positive in some specified situations, such as the control system counteracts external or internal perturbations or actuators' failures abruptly, which implies the $|s_i|$ or $\hat{\varrho}_i$ may be increase to some degree. When these states/variables are forced into the regions of $\hat{\varrho}_i > \mu$ or $|s_i| \ge \epsilon_i$, the above cases 1 and 2 will be restarting correspondingly. Thus, the boundedness of $\hat{\varrho}_i$ could be guaranteed reasonably. □

Proof of Theorem 3: Choose a positive-definite Lyapunov function candidate as

$$V_4 = \frac{1}{2}\left(\boldsymbol{s}^{\mathrm{T}}\boldsymbol{J}\boldsymbol{P}^{-1}\boldsymbol{s} + \sum_{i=1}^{3}\frac{1}{\ell_i}\bar{\varrho}_{3i}^2\right) \tag{31}$$

with $\bar{\varrho}_i = \hat{\varrho}_i - \varrho_i^*$. Differentiating V_4 and inserting the control laws, one has

$$\begin{aligned} \dot{V}_4 \le\; & -\boldsymbol{K}_3\boldsymbol{s}^2 - \boldsymbol{K}_4\boldsymbol{s}^{\mathrm{T}}\mathrm{sig}^{\gamma}(\boldsymbol{s}) \\ & + \sum_{i=1}^{3}\left(\varrho_i|s_i| - \hat{\varrho}_i|s_i| + \frac{1}{\ell_i}(\hat{\varrho}_i - \varrho_i^*)\dot{\hat{\varrho}}_i\right). \end{aligned} \tag{32}$$

In view of the dynamics equation of the adjusting parameter $\hat{\varrho}_i$ in (29), the subsequent proof process will be conducted in two cases.

Case 1. According to (29), if $|s_i| \ge \epsilon_i$, one has $\kappa_\epsilon(s_i) = 1$. Submitting the adaptive law into the above inequality (32) and adding some auxiliary equation components, it yields to

$$\begin{aligned} \dot{V}_4 \le\; & -\boldsymbol{K}_3\boldsymbol{s}^2 - \boldsymbol{K}_4\boldsymbol{s}^{\mathrm{T}}\mathrm{sig}^{\gamma}(\boldsymbol{s}) \\ & + \sum_{i=1}^{3}\left(\varrho_i|s_i| - \hat{\varrho}_i|s_i| + \varrho_i^*|s_i| - \varrho_i^*|s_i|\right) \\ & + \sum_{i=1}^{3}\left(\frac{\zeta_{1i}}{\ell_i}(\hat{\varrho}_i - \varrho_i^*)|s_i|\right) \\ & + \sum_{=1}^{3}\left(l_i(\hat{\varrho}_i - \varrho_i^*) - l_i(\hat{\varrho}_i - \varrho_i^*)\right), \end{aligned}$$

then

$$
\begin{aligned}
\dot{V}_4 \le & -\sum_{i=1}^{3}\left(k_{3i}|s_i| + k_{4i}|s_i|^{\gamma}\right)|s_i| - \sum_{i=1}^{3}\left(\varrho_i^* - \varrho_i\right)|s_i| \\
& + \sum_{i=1}^{3} l_i\left(\hat{\varrho}_i - \varrho_i^*\right) \\
& - \sum_{i=1}^{3}\left(|s_i| - \frac{\zeta_{1i}}{\ell_i}|s_i| + l_i\right)\left(\hat{\varrho}_i - \varrho_i^*\right) \\
\le & -\sum_{i=1}^{3}\left(k_{3i}|s_i| + k_{4i}|s_i|^{\gamma} + \varrho_i^* - \varrho_i\right)|s_i| \\
& - \sum_{i=1}^{3} l_i\left|\hat{\varrho}_i - \varrho_i^*\right| - \sum_{i=1}^{3}\left(\frac{\zeta_{1i}}{\ell_i}|s_i| - |s_i| - l_i\right) \\
& \times \left|\hat{\varrho}_i - \varrho_i^*\right|
\end{aligned}
$$

where $l_i > 0$ is a small constant, which is defined as an auxiliary gain for the convenience of this proof process. According to Lemma 4 proposed above, there exists a positive constant ϱ_i^* such that $\hat{\varrho}_i \le \varrho_i^*$ and $\varrho_i \le \varrho_i^*$ for all the time. Denoting

$$
\begin{aligned}
M &= \min\left\{\sqrt{2}\left(k_{3i}\epsilon_i + k_{4i}\epsilon_i^{\gamma} + \varrho_i^* - \varrho_i\right), \sqrt{2\ell_i}\, l_i\right\}, \\
\Phi_1 &= \sum_{i=1}^{3}\left(\frac{\zeta_{1i}}{\ell_i}|s_i| - |s_i| - l_i\right)\left|\hat{\varrho}_i - \varrho_i^*\right|,
\end{aligned}
$$

such that $\dot{V}_4$ follows:

$$
\dot{V}_4 \le -MV_4^{1/2} - \Phi_1 \le -MV_4^{1/2} \tag{33}
$$

if one designs appropriate values of l_i meeting the constraint $\ell_i \le (\zeta_{1i}|s_i|/|s_i| + l_i) \le (\zeta_{1i}\epsilon_i/(\epsilon_i + l_i))$ such that $\Phi_1 > 0$. Since the auxiliary parameter l_i has nothing to do with the control performances, it is always possible to choose an appropriate value of l_i to meet the above inequality constraint. Hence, the inequality (33) implies that the finite time stability of the attitude control system from any arbitrary initial conditions, converging to the limited domain $D_1 = \{s_i \| s_i| \le \epsilon_i\}$ within the finite time $T_1 \le 2V_4^{1/2}(0)/M$.

Case 2. Once the system goes into D_1, i.e. the case $|s_i| \le \epsilon_i$, we have

$$
\begin{aligned}
\dot{V}_4 \le & -\sum_{i=1}^{3}\left(k_{3i}\epsilon_i + k_{4i}\epsilon_i^{\gamma} + \varrho_i^* - \varrho\right)|s_i| \\
& - \sum_{i=1}^{3} l_i\left|\hat{\varrho}_i - \varrho_i^*\right| \\
& - \sum_{i=1}^{3}\left(-\frac{\zeta_{1i}}{\ell_i}|s_i|^{\kappa_e(s_i)} - |s_i| - l_i\right)\left|\hat{\varrho}_i - \varrho_i^*\right| \\
\le & -MV_4^{1/2} + \Phi_2 \\
\le & -MV_4^{1/2} + \Phi_2^*
\end{aligned}
\tag{34}
$$

with

$$
\Phi_2 = \sum_{i=1}^{3}\left(\frac{\zeta_{1i}}{\ell_i}|s_i|^{\kappa_e(s_i)} + |s_i| + l_i\right)\left|\hat{\varrho}_i - \varrho_i^*\right|,
$$

satisfying the constraint that

$$
\Phi_2 \le \sum_{i=1}^{3}\left(\frac{\zeta_{1i}}{\ell_i}\epsilon_i + \epsilon_i + l_i\right)\varrho_i^* \triangleq \Phi_2^*.
$$

According to the Lemma 2, the attitude control system is practical finite-time stable or finite-time uniformly ultimately bounded stable. And the convergent time satisfies the constraint $T_2 \le 2V_4^{1/2}(0)/M\theta_0, 0 < \theta_0 < 1$. On the other hand, it implies that $\dot{V}_4$ would be sign indefinite due to the existing of the term Φ_2^* in (34),

Table 1 Four failure scenarios of RWs

ith RW	e_{ii}	$\bar{\nu}_i$, Nm
$i = 1$	$\begin{cases} 1, & 0 < t < 10 \\ 0.5, & t \ge 10 \end{cases}$	0
$i = 2$	$\begin{cases} 0.85, & 100t_k < t < 50 + 100t_k \\ 0.6, & 50 + 100t_k \le t \le 100(t_k + 1) \end{cases}$	0.008
$i = 3$	$0.9 + 0.07\sin(0.2t)$	$0.05\sin(t)$
$i = 4$	$\begin{cases} 1, & 0 < t < 10 \\ 0.2, & t \ge 10 \end{cases}$	0.005

which also means that the finite time stability of the closed-loop attitude control system in the region of $|s_i| \le \epsilon_i$ may not be always guaranteed. That is, $\dot{V}_4$ may become positive value and $|s_i|$ would increase over the upper bound ϵ_i in this situation. Once $|s_i|$ goes out of the boundary, the above case 1 will be achieved with $\dot{V}_4 \le -MV_4^{1/2}$, and then V_4 starts decreasing again. Consequently, $|s_i|$ works with a stable finite time reaching dynamics, and it has a small bounded deviation of the integral-type sliding mode manifold from the domain $D_3 = \{s_i \| s_i| \le \epsilon_i\}$ during the transient response. Then, the attitude control system would converge to the bounded region as follows:

$$
D_2 = \left\{ s_i \| s_i| \le \frac{\left(\frac{\zeta_{1i}}{\ell_i}\epsilon_i + \epsilon_i + l_i\right)\varrho_i^*}{\min\left\{k_{3i}\epsilon_i + k_{4i}\epsilon_i^{\gamma} + \varrho_i^* - \delta_i\right\}} \right\}.
$$

In view of this, one can conclude that $|s_i|$ will converge to the region of D_1 in finite time, but could be sustained in the greater domain of $D_1 \cup D_2$. Therefore, with application of the FTDO mechanism in (7)–(9), the finite-time stability of the attitude control system in (1) and (4) can be established if the control laws are designed as ISMFTC in (27)–(29). □

4 Simulation and analysis

A common configuration with four RWs is chosen as the spacecraft's actuators in this example, and the configuration and assembling locations/angles are the same to the authors' previous work [16, 32]. In addition, the maximum magnitude of the output torque of the individual RW is supposed to be $\tau_{\max} = 0.25$ Nm. In order to verify the reliability of the proposed FTDO in (7)–(9) and ISMFTC in (27)–(29) in this work, four failure scenarios are firstly described mathematically in Table 1.

It is assumed that the normal moment of inertia of the rigid spacecraft is given as $\boldsymbol{J} = [20, 0, 0.9; 0, 17, 0; 0.9, 0, 15](\mathrm{kg \cdot m^2})$ according to [16, 23, 32, 41]. The initial attitude MRPs are chosen randomly as $\boldsymbol{\rho_0} = [-0.1579, 0.1368, 0.0947]^{\mathrm{T}}$, and the initial angular velocity is set as $\boldsymbol{\omega_0} = [0, 0, 0]^{\mathrm{T}}$ (rad/s). In addition, the total external disturbances are supposed as

$$
\boldsymbol{d} = 0.25 \times 10^{-3}\begin{bmatrix} 2\cos(10\varsigma t) + 3\sin(3\varsigma t) - 8 \\ -1.5\sin(2\varsigma t) + 3\cos(5\varsigma t) + 12 \\ 3\sin(10\varsigma t) - 6\sin(4\varsigma t) + 9 \end{bmatrix}(\mathrm{Nm})
$$

where ς is assumed to be $10\|\boldsymbol{\omega}\|$. And that, the gains of the proposed schemes are chosen as $\alpha_1 = 0.6$, $\lambda_1 = 1$, $\lambda_2 = 0.6$, $k_1 = 4.9$, $k_2 = 3$, $\beta_1 = 0.9$, $\gamma = 0.88$, $\zeta_{1i} = \zeta_{2i} = 0.2$, $\mu = 0.1$, $\boldsymbol{K_3} = \mathrm{diag}(6.5, 6.7, 7.2)$, $\boldsymbol{K_4} = \mathrm{diag}(4.0, 4.22, 4.0)$.

4.1 Performances of the FTDO

The time responses of observation errors of the attitude angular velocity $\boldsymbol{\omega}$ and the auxiliary variable $\boldsymbol{\xi}$ actuated by FTDO are shown in Figs. 1 and 2. As is seen in Fig. 1, the attitude angular velocity is successfully observed, and the corresponding observation error has a very high accuracy of $z_{1i} \le 2 \times 10^{-5}$ $(i = 1, 2, 3)$ during the stable status. From the time response in Fig.

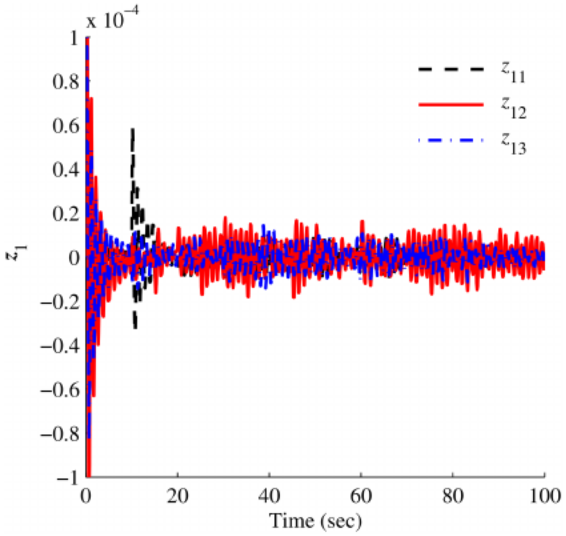

Fig. 1 *Time response of the FTDO observation errors* z_1

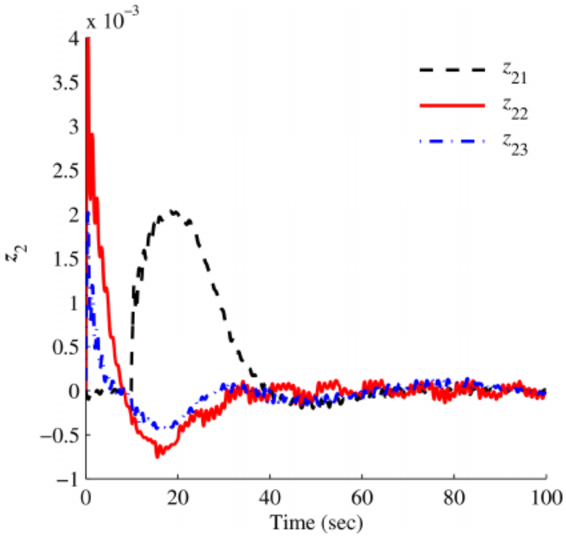

Fig. 2 *Time response of the FTDO observation errors* z_2

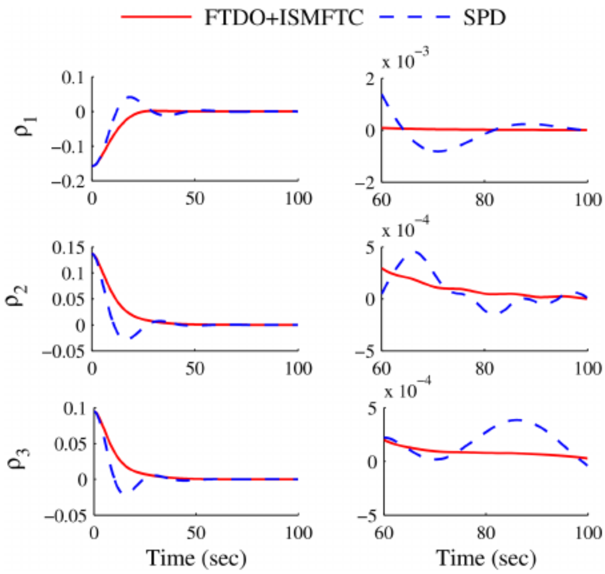

Fig. 3 *Time response of the spacecraft attitude MRPs* $\boldsymbol{\rho}$

2, it is obtained that the estimation is also achieved after the finite time, and the observation accuracy can reach $z_{2i} \leq 2 \times 10^{-5}$ $(i = 1, 2, 3)$ after 40 s. It also implies that the auxiliary variable $\boldsymbol{\vartheta}$

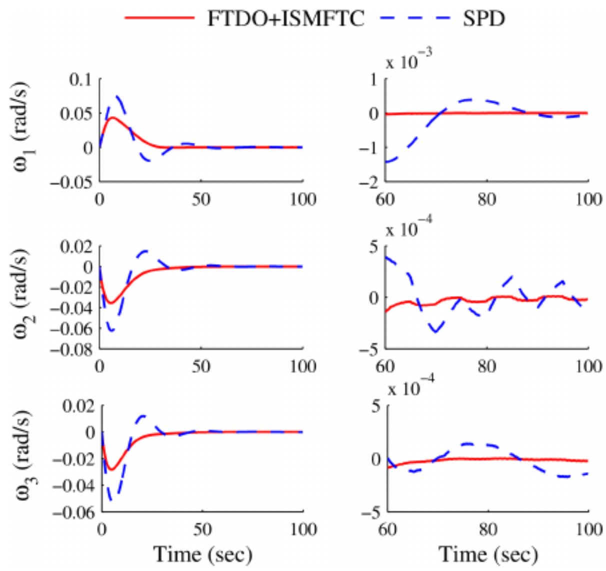

Fig. 4 *Time response of the spacecraft attitude angular velocity* $\boldsymbol{\omega}$

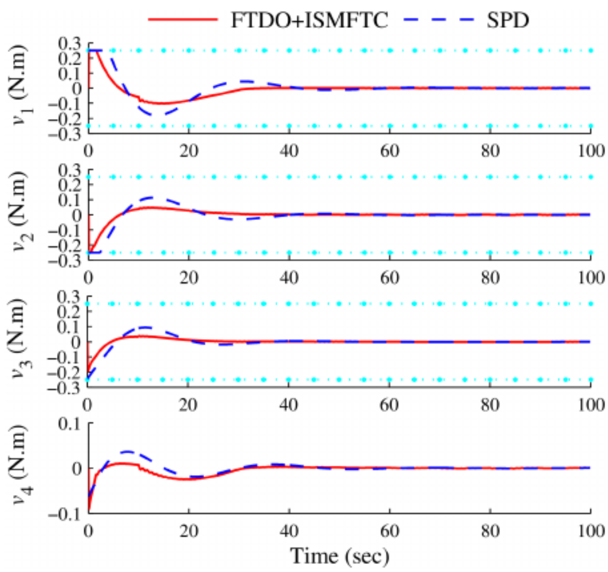

Fig. 5 *Time response of the actual actuator control torques* $\boldsymbol{v}$

is bounded, and it will converge to the synthetic uncertainty/disturbance $\bar{\boldsymbol{d}}$ in finite time.

4.2 Performances of the control schemes under actuators' partial failures

For further illustrating the effectiveness and superiority of the proposed integrated attitude control scheme FTDO+ISMFTC in this work, the saturation proportional derivative controller in [32] (noted as SPD) is conducted under the same simulation conditions for comparisons. The time responses of MRPs and attitude angular velocity are presented in Figs. 3 and 4. It is seen clearly that the proposed FTDO+ISMFTC scheme achieves fine performances with a finite settling time less than 50 sec, and a high stability accuracy of 10^{-4} for the spacecraft attitudes. What is more, the chattering phenomenon has been attenuated or restrained under the proposed control approach by using the failure/uncertainty reconstructed information deriving from the proposed FTDO. Furthermore, the time responses of the commanded actuators'/RWs' torques are presented in Fig. 5.

4.3 Performances of the control schemes under actuators' partial failures and complete failure

In this case, more severe failures of the RWs including the complete failure are considered in the simulations, and the detailed

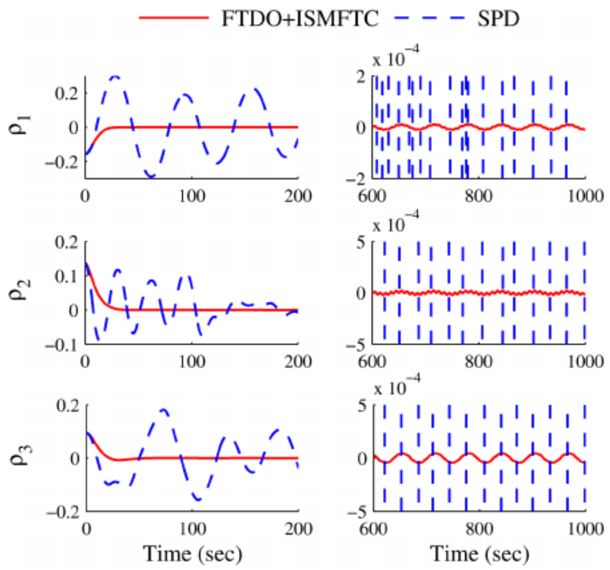

Fig. 6 *Time response of the spacecraft attitude MRPs* $\boldsymbol{\rho}$

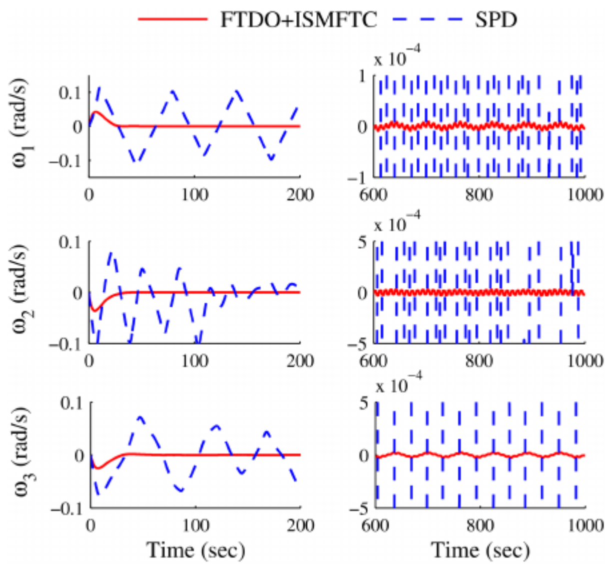

Fig. 7 *Time response of the spacecraft attitude angular velocity* $\boldsymbol{\omega}$

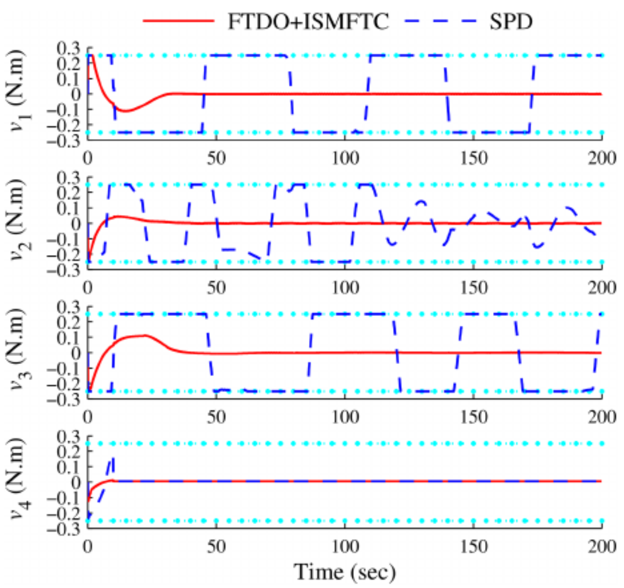

Fig. 8 *Time response of the actual actuator control torques* $\boldsymbol{v}$

failure scenarios are presented mathematically in Table 2. The time responses of MRPs and attitude angular velocity are presented in Figs. 6 and 7. It is seen clearly that the proposed FTDO+ISMFTC achieves fine performances with a finite settling time less than 70 sec with high stability accuracy. And also one can obtain that FTDO+ISMFTC manages to compensate for the actuator failures and disturbances successfully. But, the traditional PD-type control scheme SPD cannot guarantee the stability of the spacecraft attitude control system. The severe oscillations in the simulation exhibitions imply the failure of the space attitude control missions. Furthermore, the time responses of the commanded RWs' torques are presented in Fig. 8. Note that, the magnitudes of the working actuators/RWs are explicitly taken into account to meet the relevant constraints.

In brief, these above results verify that the fast convergence, high-precise attitude stabilisation and fine chattering-attenuating performance have been accomplished in the closed-loop spacecraft attitude control system by utilising the proposed approaches FTDO +ISMFTC in this work in spite of some undesired/unknown failures and disturbances.

Table 2 Four failure scenarios of RWs

*i*th RW	e_{ii}	$\bar{v}_i$, Nm
$i = 1$	$\begin{cases} 1, & 0 < t < 10 \\ 0.5, & t \geq 10 \end{cases}$	0
$i = 2$	$\begin{cases} 0.85, & 100t_k < t < 50 + 100t_k \\ 0.6, & 50 + 100t_k \leq t \leq 100(t_k + 1) \end{cases}$	0.008
$i = 3$	$0.2 + 0.07\sin(0.2t)$	$0.05\sin(t)$
$i = 4$	$\begin{cases} 1, & 0 < t < 10 \\ 0, & t \geq 10 \end{cases}$	0.005

5 Conclusion

In this paper, a novel FTDO incorporating with an integral sliding mode based fault tolerant attitude control scheme is developed for a rigid spacecraft, which is subject to external disturbance torques and actuator failures. Firstly, a simple and novel FTDO is designed to reconstruct the synthetic uncertainty deriving form actuator failures and disturbances. Using the observations obtained by FTDO, an integral sliding mode based finite-time fault tolerant attitude stabilisation controller integrating with an adjusting law is investigated to ensure the closed-loop attitude control system converge to the stable region in finite time. However, the designed FTDO only provides the so-called synthetic/lumped uncertainty/disturbance, rather than isolates and identifies the individual failure of the actuators, which is one of the subjects in our future researches.

6 Acknowledgments

This work was supported in part by the National Natural Science Foundation of China (grant nos. 61703272, 61633003), and Shanghai Science and Technology Commission (grant nos. 17595810300, 18295801100).

7 References

[1] Shen, Q., Yue, C., Goh, C.H.: 'Velocity-free attitude reorientation of a flexible spacecraft with attitude constraints', *J. Guid. Control Dyn.*, 2017, **40**, (5), pp. 1293–1299

[2] Sharma, R., Tewari, A.: 'Optimal nonlinear tracking of spacecraft attitude maneuvers', *IEEE Trans. Control Syst. Technol.*, 2004, **12**, (5), pp. 677–682

[3] Tiwari, P.M., Janardhanan, S., Nabi, M.U.: 'Rigid spacecraft attitude control using adaptive integral second order sliding mode', *Aerosp. Sci. Technol.*, 2015, **42**, pp. 50–57

[4] Li, B., Hu, Q., Qi, J.: 'Null-space-based optimal control reallocation for spacecraft stabilization under input saturation', *Int. J. Adapt. Control Signal Process.*, 2015, **29**, (6), pp. 705–724

[5] Xin, M., Pan, H.: 'Indirect robust control of spacecraft via optimal control solution', *IEEE Trans. Aerosp. Electron. Syst.*, 2012, **48**, (2), pp. 1798–1809

[6] Cao, X., Wu, B.: 'Indirect adaptive control for attitude tracking of spacecraft with unknown reaction wheel friction', *Aerosp. Sci. Technol.*, 2015, **47**, pp. 493–500

[7] Bai, H., Zhou, Y., Sun, H., *et al.*: 'Observer-based non-linear H_∞ attitude control for a flexible satellite', *IET Control Theory Appl.*, 2017, **11**, (15), pp. 2403–2411

[8] Xiao, B., Hu, Q., Zhang, Y.: 'Finite-time attitude tracking of spacecraft with fault-tolerant capability', *IEEE Trans. Control Syst. Technol.*, 2015, **23**, (4), pp. 1338–1350

[9] Bustan, D., Pariz, N., Hosseini Sani, S.K.: 'Robust fault-tolerant tracking control design for spacecraft under control input saturation', *ISA Trans.*, 2014, **53**, (4), pp. 1073–1080

[10] Lee, H., Kim, Y.: 'Fault-tolerant control scheme for satellite attitude control system', *IET Control Theory Appl.*, 2010, **4**, (8), pp. 1436–1450

[11] Lee, D., Kumar, K.D., Sinha, M.: 'Fault detection and recovery of spacecraft formation flying using nonlinear observer and reconfigurable controller', *Acta Astronaut.*, 2014, **97**, (1), pp. 58–72

[12] Xiao, B., Yin, S., Gao, H.: 'Reconfigurable tolerant control of uncertain mechanical systems with actuator faults: A sliding mode observer-based approach', *IEEE Trans. Control Syst. Technol.*, 2018, **26**, (4), , pp. 1249–1258, doi: 10.1109/TCST.2017.2707333

[13] Daly, J., Wang, D: 'Output feedback sliding mode control in the presence of unknown disturbances', *Syst. Control Lett.*, 2009, **58**, (3), pp. 188–193

[14] L'Afflitto, A., Mohammadi, K.: 'Robust observer-based control of nonlinear dynamical systems with state constraints', *J. Franklin Inst.*, 2017, **354**, (16), pp. 7385–7409

[15] Li, B., Hu, Q., Ma, G.: 'Extended state observer based robust attitude control of spacecraft with input saturation', *Aerosp. Sci. Technol.*, 2016, **50**, pp. 173–182

[16] Li, B., Hu, Q., Yu, Y.*, et al.*: 'Observer-based fault tolerant attitude control for rigid spacecraft', *IEEE Trans. Aerosp. Electron. Sys.*, 2017, **53**, (5), pp. 2572–2582

[17] Yang, J., Li, S., Sun, C.*, et al.*: 'Nonlinear disturbance observer based robust flight control for airbreathing hypersonic vehicles', *IEEE Trans. Aerosp. Electron. Syst.*, 2013, **49**, (2), pp. 1263–1275

[18] Besnard, L., Shtessel, Y.B., Landrum, B.: 'Quadrotor vehicle control via sliding mode controller driven by sliding mode disturbance observer', *J. Franklin Inst.*, 2012, **349**, (2), pp. 658–684

[19] Lee, K., Back, J., Choy, I.: 'Nonlinear disturbance observer based robust attitude tracking controller for quadrotor UAVs', *Int. J. Control Autom. Syst.*, 2014, **12**, (6), pp. 1266–1275

[20] Sun, L., Zheng, Z.: 'Disturbance observer-based robust backstepping attitude stabilization of spacecraft under input saturation and measurement uncertainty', *IEEE Trans. Ind. Electron.*, 2017, **64**, (10), pp. 7994–8002

[21] Mokhtari, M.R., Cherki, B., Braham, A.C.: 'Disturbance observer based hierarchical control of coaxial-rotor UAV', *ISA Trans.*, 2017, **67**, pp. 466–475

[22] Bhat, S.P., Bernstein, D.S.: 'Finite-time stability of continuous autonomous systems', *SIAM J. Control Optim.*, 2000, **38**, (3), pp. 751–766

[23] Zou, A.: 'Finite time output feedback attitude tracking control for rigid spacecraft', *IEEE Trans. Control Syst. Technol.*, 2014, **22**, (1), pp. 338–345

[24] Hong, Y., Xu, Y., Huang, J.: 'Finite-time control for robot manipulators', *Syst. Control Lett.*, 2002, **46**, (4), pp. 243–253

[25] Du, H., Li, S.: 'Finite-time attitude stabilization for a spacecraft using homogeneous method', *J. Guid. Control Dyn.*, 2012, **35**, (3), pp. 740–748

[26] Gui, H., Jin, L., Xu, S.: 'Simple finite-time attitude stabilization laws for rigid spacecraft with bounded inputs', *Aerosp. Sci. Technol.*, 2015, **42**, pp. 176–186

[27] Utkin, V., Guldner, J., Shi, J.: '*Sliding mode control in electromechanical systems*' (Taylor & Francis, London, UK, 1999)

[28] Hamayun, M.T., Edwards, C., Alwi, H.: 'Design and analysis of an integral sliding mode fault-tolerant control scheme', *IEEE Trans. Autom. Control*, 2012, **57**, (7), pp. 1783–1789

[29] Liang, Y.W., Ting, L.W., Lin, L.G.: 'Study of reliable control via an integral-type sliding mode control scheme', *IEEE Trans. Ind. Electron.*, 2012, **59**, (8), pp. 3062–3068

[30] Shen, Q., Wang, D., Zhu, S.*, et al.*: 'Integral-type sliding mode fault-tolerant control for attitude stabilization of spacecraft', *IEEE Trans. Control Syst. Technol.*, 2015, **23**, (3), pp. 1131–1138

[31] Gui, H., Vukovich, G.: 'Adaptive fault-tolerant spacecraft attitude control using a novel integral terminal sliding mode', *Int. J. Robust Nonlinear Control*, 2017, doi: 10.1002/rnc.3733

[32] Hu, Q., Li, B., Zhang, Y.: 'Nonlinear proportional derivative control incorporating closed-loop control allocation for spacecraft', *J. Guid. Control Dyn.*, 2014, **37**, (3), pp. 799–812

[33] Hughes, P.C.: '*Spacecraft attitude dynamics*' (Wiley, New York, 2004), p. p 59

[34] Xiao, B., Hu, Q., Zhang, Y.*, et al.*: 'Fault-tolerant tracking control of spacecraft with attitude-only measurement under actuator failures', *J. Guid. Control Dyn.*, 2014, **37**, (3), pp. 838–849

[35] Zhu, Z., Xia, Y., Fu, M.: 'Attitude stabilization of rigid spacecraft with finite-time convergence', *Int. J. Robust Nonlinear Control*, 2011, **21**, (6), pp. 686–702

[36] Hu, Q., Jiang, B.: 'Continuous finite-time attitude control for rigid spacecraft based on angular velocity observer', *IEEE Trans. Aerosp. Electron. Syst.*, 2018, **54**, (3), pp. 1082–1092

[37] Hu, Q., Jiang, B., Zhang, Y.: 'Observer-based output feedback attitude stabilization for spacecraft with finite-time convergence', *IEEE Trans. Control Syst. Technol.*, 2017, doi: 10.1109/TCST.2017.2780061

[38] Rubagotti, M., Estrada, A., Castanos, F.*, et al.*: 'Integral sliding mode control for nonlinear systems with matched and unmatched perturbations', *IEEE Trans. Autom. Control*, 2011, **56**, (11), pp. 2699–2704

[39] Wang, L., Sheng, Y., Liu, X.: 'A novel adaptive high-order sliding mode control based on integral sliding mode', *Int. J. Control Autom. Syst.*, 2014, **12**, (3), pp. 459–472

[40] Plestan, F., Shtessel, Y., Brégeault, V.*, et al.*: 'New methodologies for adaptive sliding mode control', *Int. J. Control*, 2010, **83**, (9), pp. 1907–1919

[41] Cai, W., Liao, X., Song, D.: 'Indirect robust adaptive fault-tolerant control for attitude tracking of spacecraft', *J. Guid. Control Dyn.*, 2012, **31**, (5), pp. 1456–1463